JOURNAL OF MAGNETIC RESONANCE 87, 584–591 (1990)

# NOTES

## A Novel $^{15}N$ Chemical-Shift NMR Thermometer for Magic Angle Spinning Experiments

BERND WEHRLE, FRANCISCO AGUILAR-PARRILLA, AND HANS-HEINRICH LIMBACH

*Institut für Physikalische Chemie der Universität, Albertstrasse 21, D-7800 Freiburg i. Br., West Germany*

Received July 18, 1989; revised September 22, 1989

Variable temperature CPMAS NMR spectroscopy (cross polarization magic angle spinning) has become a valuable tool for elucidating molecular structure and dynamics in the solid state (*1, 2*). Precise temperature measurement is of prime importance for the success of this method. Generally, it is assumed that the sample temperature is equal to the temperature of the inlet sample driving and bearing gas and that there is no temperature gradient across the sample. This assumption is justified when small rotors are employed and when the thermometer is placed very close to the sample. In other cases this procedure may, however, lead to temperature calibration errors (*3*). Therefore, the indirect measurement of temperature via the observation of temperature-induced spectral changes due to solid–solid phase transitions or temperature-dependent chemical shifts is often more reliable. Whereas the use of a phase-transition thermometer is suitable for calibrating a conventional thermometer at a given phase-transition temperature (*4*), chemical-shift NMR thermometers can be employed in a large temperature range. For $^{13}C$ CPMAS NMR measurements a thermometer based on the Curie law behavior of the $^{13}C$ chemical shifts of paramagnetic samarium acetate tetrahydrate (SAT) has been proposed (*5, 6*). However, an unfavorable ratio, for this material, of temperature-induced line shifts to the signal linewidth, especially in and above room temperature, make the development of improved chemical-shift thermometers for MAS studies desirable.

We present here a $^{15}N$ CPMAS chemical-shift thermometer with a resolution of about $\pm 2$ K, based on the tautomerism of an organic dye molecule TTAA,[1] shown in Fig. 1. The reaction network of Fig. 1 has been established previously (*7, 8*). Because of the low natural abundance and sensitivity of the $^{15}N$ nucleus, TTAA was artifically enriched to about 95% with $^{15}N$, as has been described recently (*8*). The $^{15}N$ CPMAS spectra were measured using an electromagnet with a magnetic field of 2.1 T corresponding to a $^{15}N$ Larmor frequency of 9.12 MHz and a 5 mm Doty MAS probe (*9*) together with a homebuilt heat exchanger (*10*). The corresponding temperatures were measured with a Pt resistance thermometer (dimensions: 2.3 $\times$ 2.1 mm, Degussa), which was positioned approximately 3 mm from RF coil in the

[1] TTAA, 1,8-dihydro-5,7,12,14-tetramethyldibenzo(*b,i*)-1,4,8,11-tetraazacyclotetradeca-4,6,11,13-tetraene-$^{15}N_4$ (tetramethyldibenzotetraaza(14)annulene).

0022-2364/90 $3.00

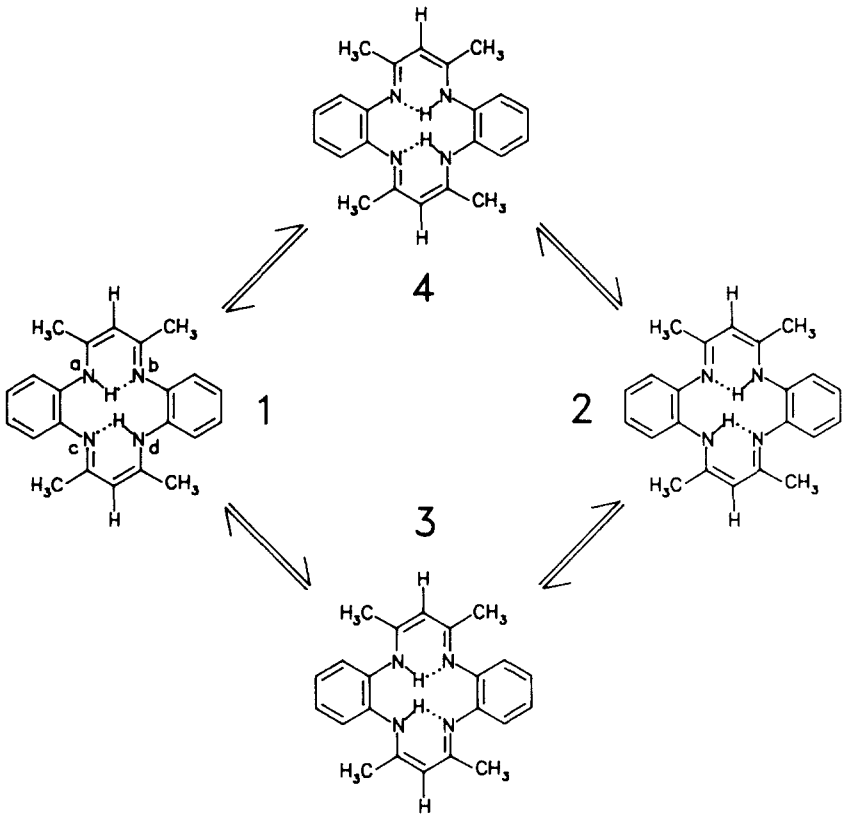


FIG. 1. The tautomerism of TTAA according to Ref. (*7*).

inlet gas stream. No RF coil pickup could be detected during the duty cycle. Using this Pt resistance thermometer, the solid-phase transition of 1,4-diazabicyclo-[2,2,2]-octane at 351 K (*4*) could be reproduced within ±1 K.

Figure 2 shows the $^{15}N$ CPMAS NMR spectra of crystalline TTAA in the temperature range between 86 and 405 K. Only 100 scans were needed per spectrum in order to achieve a good signal-to-noise ratio. As described previously (*7*) four lines *a* to *d* are observed with temperature-dependent line separations $\delta_{ab} = \delta_a - \delta_b$ and $\delta_{dc} = \delta_d - \delta_c$ which are shown in Table 1. $^{15}N$ spin-diffusion measurements showed that this observation is due to the fact that each TTAA molecule contains four chemically inequivalent nitrogen atoms *a* to *d* characterized by different temperature-dependent average proton densities (*7*).

The variation of the splittings $\delta_{mn}$ between the lines $mn = ab$ and $dc$ as a function of temperature was obtained in a quantitative way on the basis of the reaction network in Fig. 1 as follows. Due to solid-state effects the gas-phase degeneracies between the tautomeric states 1 and 2 as well as between 3 and 4 are lifted. The single reaction steps in Fig. 1 are characterized by the equilibrium constants (*7*)

$$K_{ij} = C_j/C_i = \exp(-\Delta H_{ij}/RT + \Delta S_{ij}/R), \qquad [1]$$

where $C_i$ is the concentration of the tautomeric state $i$, $T$ the temperature, and $R$ the

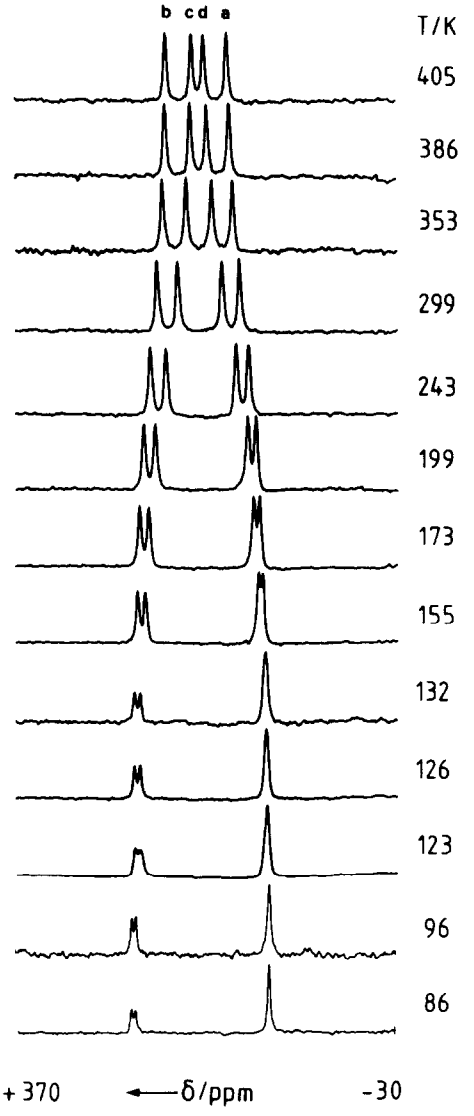


FIG. 2. $^{15}N$ CPMAS NMR spectra of 95% $^{15}N$-enriched TTAA at 9.12 MHz as a function of temperature; 6–10 ms cross-polarization time, 7 kHz spectral width, 2.7 s repetition time, 100 scans on average, 2–2.8 kHz rotation frequency, single nitrogen gas supply for sample bearing and driving.

gas constant. $\Delta S_{ij}$ and $\Delta H_{ij}$ are the reaction entropy and reaction enthalpy of the reaction step $ij$. The line separations $\delta_{mn}$ are functions of the average proton density ratios

$$K_{ab} = (C_2 + C_4)/(C_1 + C_3) = (K_{12} + K_{14})/(1 + K_{13}) \qquad [2]$$

TABLE 1

Chemical-Shift Difference of the $^{15}N$ Signals of TTAA as a Function of Temperature Measured at 9.12 MHz Using a Doty Double-Bearing Spinner Design

| $T$ [K] | $\delta\nu_{ab}$ [ppm] | $K_{ab}$ | $\delta\nu_{dc}$ [ppm] | $K_{dc}$ |
|---|---|---|---|---|
| 123 | 138.7 | 0.017 | 132.7 | 0.028 |
| 126 | 137.9 | 0.019 | 131.9 | 0.031 |
| 132 | 137.2 | 0.022 | 131.3 | 0.034 |
| 155 | 130.4 | 0.047 | 118.4 | 0.085 |
| 160 | 129.5 | 0.051 | 116.7 | 0.092 |
| 172 | 125.9 | 0.065 | 110.9 | 0.118 |
| 173 | 125.3 | 0.067 | 109.2 | 0.125 |
| 181 | 123.1 | 0.076 | 104.9 | 0.144 |
| 182 | 121.9 | 0.081 | 104.8 | 0.145 |
| 189 | 120.6 | 0.086 | 103.3 | 0.152 |
| 191 | 120.0 | 0.089 | 100.3 | 0.167 |
| 199 | 116.8 | 0.102 | 96.4 | 0.186 |
| 202 | 116.1 | 0.105 | 95.1 | 0.193 |
| 243 | 103.3 | 0.163 | 73.9 | 0.310 |
| 250 | 100.2 | 0.177 | 69.3 | 0.339 |
| 299 | 86.8 | 0.246 | 46.7 | 0.500 |
| 313 | 83.7 | 0.263 | 41.5 | 0.544 |
| 324 | 79.9 | 0.284 | 37.7 | 0.577 |
| 334 | 78.4 | 0.293 | 34.0 | 0.611 |
| 344 | 76.2 | 0.306 | 30.1 | 0.647 |
| 353 | 73.9 | 0.320 | 27.2 | 0.676 |
| 360 | 72.4 | 0.329 | 24.8 | 0.700 |
| 366 | 71.6 | 0.334 | 23.4 | 0.715 |
| 374 | 70.2 | 0.343 | 20.4 | 0.747 |
| 386 | 67.1 | 0.363 | 17.3 | 0.780 |
| 397 | 65.6 | 0.372 | 14.3 | 0.815 |
| 405 | 64.0 | 0.383 | 12.8 | 0.833 |

Low temperature splitting at 86 K:
$\Delta\nu_{ab}$ = 143.4 [ppm] $\Delta\nu_{dc}$ = 140.5 [ppm]

and

$$K_{dc} = (C_2 + C_3)/(C_1 + C_4) = (K_{12} + K_{13})/(1 + K_{14}). \quad [3]$$

Thus, it can easily be shown (*7*) that

$$\delta_{mn} = \Delta_{mn}(1 - K_{mn})/(1 + K_{mn}), \qquad mn = ab, dc, \quad [4]$$

i.e.,

$$K_{mn} = (1 - \delta_{mn}/\Delta_{mn})/(1 + \delta_{mn}/\Delta_{mn}), \qquad mn = ab, dc. \quad [5]$$

The intrinsic chemical-shift difference of atoms $m$ and $n$ obtained at low temperature, where $K_{mn} \approx 0$, is $\Delta_{mn}$. By combination of Eqs. [1]–[3] it follows that

TABLE 2

Temperature-Induced Chemical-Shift Changes $d\delta/dT$ in [ppm/K] of TTAA and Samarium Acetate Tetrahydrate (SAT) (5)

| $T$[K] | TTAA[a] | TTAA[b] | SAT[c] |
|---|---|---|---|
| 90 | 0.110 | 0.060 | 0.601 |
| 110 | 0.231 | 0.130 | 0.402 |
| 130 | 0.357 | 0.205 | 0.288 |
| 150 | 0.457 | 0.267 | 0.216 |
| 200 | 0.549 | 0.330 | 0.122 |
| 250 | 0.495 | 0.303 | 0.078 |
| 300 | 0.404 | 0.250 | 0.054 |
| 350 | 0.320 | 0.200 | 0.040 |
| 400 | 0.253 | 0.159 | 0.030 |

[a] *dc* line pair calculated from Eq. [12].
[b] *ab* line pair calculated from Eq. [11].
[c] Calculated from Ref. (5).

$$\ln K_{ab} = \ln\{\exp(-\Delta H_{12}/RT + \Delta S_{12}/R) + \exp(-\Delta H_{14}/RT + \Delta S_{14}/R)\} - \ln\{1 + \exp(-\Delta H_{13}/RT + \Delta S_{13}/R)\} \quad [6]$$

and that

$$\ln K_{dc} = \ln\{\exp(-\Delta H_{12}/RT + \Delta S_{12}/R) + \exp(-\Delta H_{13}/RT + \Delta S_{13}/R)\} - \ln\{1 + \exp(-\Delta H_{14}/RT + \Delta S_{14}/R)\}. \quad [7]$$

The line positions (Table 1) were analyzed as follows. First, the $K_{ab}$ and $K_{dc}$ values listed in Table 1 were calculated using Eq. [5] and the low temperature splittings $\Delta_{ab}$ = 143.4 ppm and $\Delta_{dc}$ = 140.5 ppm. Then, a simultaneous nonlinear least-squares fit of the experimental ln $K_{ab}$ and ln $K_{dc}$ values vs $1/T$ was performed, which allowed the determination of the parameters in Eqs. [6] and [7]. The result of this fit was very satisfactory as shown in Fig. 3. We obtained $\Delta H_{12}$ = 4.94 kJ mol$^{-1}$, $\Delta S_{12}$ = 6.47 J K$^{-1}$ mol$^{-1}$, $\Delta H_{13}$ = 4.65 kJ mol$^{-1}$, $\Delta S_{13}$ = 2.25 J K$^{-1}$ mol$^{-1}$, and $\Delta H_{14} \gg 0$. In other words, between 100 and 400 K,

$$K_{12} = 2.18\exp(-594/T), \qquad K_{13} = 1.31\exp(-560/T), \qquad K_{14} \approx 0. \quad [8]$$

This result can be interpreted as follows: the most stable form is the trans form 1 in Fig. 1; due to solid-state effects the second trans form 2 has a higher energy than 1. The energy of the cis form 3 has approximately the same energy as form 2; the cis tautomer 4 is not populated to an observable extent.

Combining Eqs. [2]–[4] with Eq. [8] we obtain the following simple equations for the temperature dependence of the TTAA $^{15}$N line splittings:

$$\delta_{ab} = \Delta_{ab}\frac{1 - 2.18\exp(-595/T) + 1.31\exp(-560/T)}{1 + 2.18\exp(-595/T) + 1.31\exp(-560/T)}, \quad \Delta_{ab} = 143.4 \text{ ppm}, \quad [9]$$

$$\delta_{dc} = \Delta_{dc}\frac{1 - 2.18\exp(-595/T) - 1.31\exp(-560/T)}{1 + 2.18\exp(-595/T) + 1.31\exp(-560/T)}, \quad \Delta_{dc} = 140.5 \text{ ppm}. \quad [10]$$

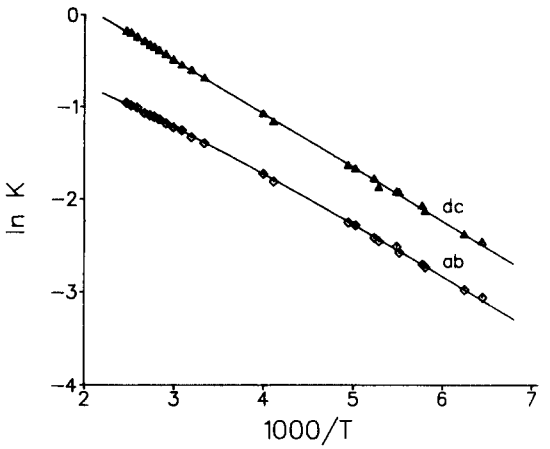


FIG. 3. Simultaneous nonlinear least-squares fit in terms of Eqs. [6] and [7] of the experimental ln $K_{ab}$ and ln $K_{dc}$ values vs $1/T$.

For a better understanding, the theoretical values of $\delta_{ab}/\Delta_{ab}$ and $\delta_{dc}/\Delta_{dc}$ calculated according to these equations are plotted in Fig. 4 as a function of temperature. In order to discuss these curves let us, furthermore, differentiate Eqs. [9] and [10] vs temperature. We obtain

$$d\delta_{ab}/dT = -3.72 \times 10^5 T^{-2} \frac{\exp(-595/T) + 0.0771 \exp(-560/T)}{[1 + 2.18 \exp(-595/T) + 1.31 \exp(-560/T)]^2} \quad [11]$$

$$d\delta_{dc}/dT = -3.645 \times 10^5 T^{-2} \times \frac{\exp(-595/T) + 0.5656 \exp(-560/T)}{[1 + 2.18 \exp(-595/T) + 1.31 \exp(-560/T)]^2}. \quad [12]$$

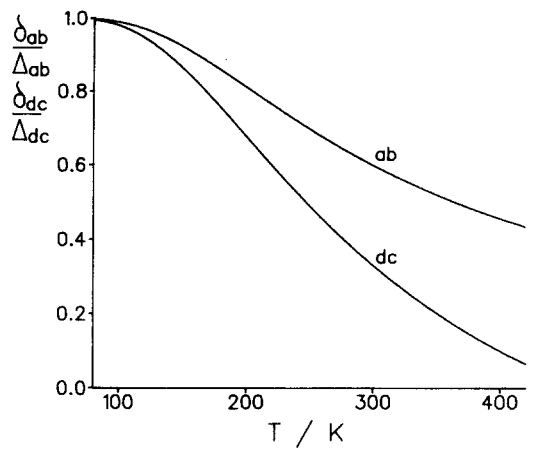


FIG. 4. Theoretical values of the relative line separations $\delta_{ab}/143.4$ and $\delta_{dc}/140.5$ as a function of temperature calculated according to Eqs. [9] and [10].

Values of the latter quantities are compared in Table 2 together with those calculated for the SAT thermometer (*5*).

Taking into account the fact that the linewidths of the spectra in Fig. 2 are typically of the order of 4.4 ppm including artificial line broadening—which is slightly better than those of the SAT $^{13}C$ lines (*5*) where we estimate values of about 5 ppm—it follows from Fig. 4 and Table 2 that below 120 K the TTAA thermometer is less accurate than the SAT thermometer. By contrast, above 130 K the TTAA thermometer is superior. From Table 2 and Fig. 4 it follows that the temperature dependence of $\delta_{dc}$ is stronger than that of $\delta_{ab}$. Therefore, it is more precise to determine $T$ from $\delta_{dc}$ of the inner TTAA lines rather than from the splitting $\delta_{ab}$ of the outer lines. The maximum sensitivity of the TTAA thermometer is reached at 199 K where $d\delta_{dc}/d_{dc} = 0.55$ ppm/K. Although experiments were performed here only up to 405 K the TTAA thermometer can, in principle, also be employed at higher temperatures, the melting point of TTAA being 502 K (*7*).

The margin of error of the TTAA thermometer and its capability to detect temperature gradients can be estimated as follows. If one calculates the temperature $T$ using the experimental $\delta_{dc}$ values in Table 1 and compares it with the experimental $T$ values a statistical temperature error of ±2 K results. The margin of error is, however, not uniform in the whole temperature range, as indicated by Table 2. Estimating that the line position error is approximatively 1/10 of the linewidth, i.e., 0.4 ppm, it follows that the margin of error is less than ±1 around 200 K, ±1 at room temperature, and ±2 K at 130 and 400 K, which does not yet include an absolute temperature calibration error of ±1 K. Note that the resolution of the TTAA thermometer is enhanced when working with superconducting high field magnets. Preliminary 30.41 MHz $^{15}N$ CPMAS experiments on TTAA at 7.1 T show that the linewidths are reduced to 2.3 ppm indicating that a substantial part of the linewidths of the spectra in Fig. 2 may be due to the inhomogeneity of the magnetic field. Thus, at higher magnetic fields the margin of error of the TTAA thermometer may be reduced to below ±1 K. Note that a temperature gradient of 5 K in the sample would lead to an easily detectable line broadening between 1.3 and 2.7 ppm.

One further advantage of the TTAA thermometer is that internal reference of the line positions is provided in contrast to SAT where chemical shifts are referenced to TMS. The determination of the Larmor frequency of the latter in a separate experiment will introduce a small error absent in the TTAA case.

In conclusion, we have described a $^{15}N$ CPMAS NMR thermometer with a resolution of approximatively ±2 K which might be of use in variable temperature experiments. We are currently checking the related porphycene molecule (*11*) whose solid-state tautomerism leads to spectral changes similar to those of the TTAA tautomerism for use below 100 K.

## ACKNOWLEDGMENTS

This work was supported by the Stiftung Volkswagenwerk, Hannover; the Bundesministerium für Forschung und Technologie, Bonn; and the Fonds der Chemischen Industrie, Frankfurt.

## REFERENCES


1. C. A. FYFE, "Solid State NMR for Chemists," C.F.C. Press, Guelph, Ontario, 1983.
2. J. R. LYERLA, C. S. YANNONI, AND C. A. FYFE, *Acc. Chem. Res.* **15,** 208 (1982).
3. A. D. ENGLISH, *J. Magn. Reson.* **57,** 491 (1984).
4. J. F. HAW, R. A. CROOK, AND R. C. CROSBY, *J. Magn. Reson.* **66,** 551 (1986).
5. G. C. CAMPBELL, R. C. CROSBY, AND J. F. HAW, *J. Magn. Reson.* **69,** 191 (1986).
6. J. F. HAW, G. C. CAMPBELL, AND R. C. CROSBY, *Anal. Chem.* **58,** 3172 (1986).
7. H. H. LIMBACH, B. WEHRLE, H. ZIMMERMANN, R. D. KENDRICK, AND C. S. YANNONI, *J. Am. Chem. Soc.* **109,** 929 (1987).
8. B. WEHRLE, H. ZIMMERMANN, AND H. H. LIMBACH, *J. Am. Chem. Soc.* **109,** 929 (1988).
9. R. D. KENDRICK, S. FRIEDRICH, B. WEHRLE, H. H. LIMBACH, AND C. S. YANNONI, *J. Magn. Reson.* **65,** 159 (1985).
10. F. D. DOTY AND P. D. ELLIS, *Rev. Sci. Instrum.* **52,** 1868 (1981).
11. B. WEHRLE, H. H. LIMBACH, M. KÖCHER, O. ERMER, AND E. VOGEL, *Angew. Chem.* **99,** 914 (1987); *Angew. Chem. Int. Ed. Engl.* **26,** 934 (1987).